



HAL
open science

Longtime solar performance estimations of low-E glass depending on local atmospheric conditions

Antoine Grosjean, Estelle Le Baron

► **To cite this version:**

Antoine Grosjean, Estelle Le Baron. Longtime solar performance estimations of low-E glass depending on local atmospheric conditions. *Solar Energy Materials and Solar Cells*, 2022, 240, pp.111730. 10.1016/j.solmat.2022.111730 . cea-04574332

HAL Id: cea-04574332

<https://cea.hal.science/cea-04574332>

Submitted on 22 Jul 2024

HAL is a multi-disciplinary open access archive for the deposit and dissemination of scientific research documents, whether they are published or not. The documents may come from teaching and research institutions in France or abroad, or from public or private research centers.

L'archive ouverte pluridisciplinaire **HAL**, est destinée au dépôt et à la diffusion de documents scientifiques de niveau recherche, publiés ou non, émanant des établissements d'enseignement et de recherche français ou étrangers, des laboratoires publics ou privés.



Distributed under a Creative Commons Attribution - NonCommercial 4.0 International License

Longtime Solar Performance estimations of low-E glass depending on Local Atmospheric Conditions

Antoine Grosjean¹, Estelle Le Baron^{2*}

¹ Univ. Grenoble Alpes, G-SCOP, F-38000 Grenoble, France

² Univ. Grenoble Alpes, CEA, Liten, LITEN, DTCH, L2TS, F-38000 Grenoble, France

* Corresponding author: estelle.lebaron@cea.fr

Abstract.

In the construction industry, low-emissivity glass is used to improve both thermal efficiency and visual comfort by reflecting or transmitting thermal radiation. The solar optical performances of this type of glass are calculated using the ASTM G173 (AM 1.5) solar spectrum, the unique worldwide standard. However, the local atmospheric conditions of real sites around the world are different from those used to model the ASTM solar spectrum, originally created for PV deployment in North America in the 2000s. As the latter has an impact on the shape of the ground-based solar spectra, the real solar properties of the installed low-e glass can be different from those calculated in laboratory conditions and using the standard. In this paper, we provide a comprehensive, multi-years analysis of the solar performances of a complete set of low-e glass located on 12 sites around the world. Local solar spectra are modeled using local atmospheric data. This new study analyse the solar transmittance of low-e glass around the world. Our results show that the ASTM solar spectrum is appropriate for the majority of the selected locations. For some particular sites, such as buildings near the equator or located in cities with high atmospheric turbidity, the standard solar spectrum is not appropriate. For these sites, solar transmittance can vary up to 5% when compared to the ASTM standard. Consequently, this paper shows the necessity to include the impact of local atmospheric conditions on the performances of low-e glass.

Keywords: low-e coating, solar control, smart windows, atmospheric conditions

Nomenclature

AM: Air Mass value

AOD: Aerosol Optical Depth

A_s: Solar absorptance

A_{s,lt}: Longtime solar absorptance

ASTM G173: Solar spectra used as standard

DNI: Direct Normal Irradiance in W.m⁻²

GHI: Global Horizontal Irradiation in kWh.m ⁻²
GTI: Global Irradiance on a tilted surface in W.m ⁻²
Irr: Irradiance, in W.m ⁻²
pp: Percentage point
PW: Precipitable Water, in cm
T _s : Solar transmittance
T _{s,it} : Longtime solar transmittance
SHGC: Solar Heat Gain Coefficient
α ₁ and α ₂ : Angström coefficients
ε: Thermal emissivity

1. Introduction

Since time immemorial, man has strived to build and develop comfortable shelters to live in. Historically, fire and solar energy have been the main energy supplies produced to maintain a comfortable interior living environment. Thus, even before the democratization of glass windows, the number, orientation and shape of exterior openings have been studied with the objective of controlling solar gain so as to maintain optimum inside temperatures over the seasons. Therefore, people have always sought to optimise solar energy.

When glass became the standard for the construction of buildings, solar radiation became possible; heat and light could enter into protected environments. Comfortable living and working spaces were created thanks to the daylight and solar heat which passed through the glass. As the use of glass structures in buildings became increasingly widespread over the years. The optical properties of the glass used, and thus its solar performance became crucial. This has been even more emphasized by the increasing trend to use wide glass surfaces in today's buildings. Several factors, such as quantity and quality of light, glare reduction, optimum lighting conditions and a satisfactory view from the inside, are taken into consideration when glass and windows are chosen [1], [2]. In addition, there are energy considerations. Indeed, buildings throughout the world consume huge amounts of energy to maintain optimal inside temperatures, either by heating or air conditioning. Even though our study was not exhaustive, we observe that the energy consumption of residential and commercial buildings in developed countries is particularly high. The energy bill of these buildings represents between 20% and 40% of the total national energy consumption, depending on the country [3], [4], [5]. This number often exceeds the energy consumption needed in the transport and industry sectors [6]. A significant part of this energy use is directly related to the windows, leading to heat loss in cold climates, or over-abundant solar capture in warm ones, which increases heat and air-conditioning expenses [7], depending on the location of the buildings.

Furthermore, we have deduced that the ideal window should ensure a good visual comfort by transmitting the visible solar spectrum, mainly from 400 to 700 nm [8]. Ideally, UV rays (280-400 nm) should be reflected towards the outside so as to preserve people's health and protect the inside materials from negative aging effects, such as surface discolouration [9], [10]. Regarding the treatment of infrared radiations (700-2500 nm, 50% of the total solar flux), the ideal optical curves of a smart window are often contradictory and depend on the climate [11]. Indeed,

depending on the outside temperature and the site insulation, the sun's infrared radiation can be either beneficial (free solar energy gain) or detrimental (increase in both the heating and air conditioning costs) [12], [13]. These “smart windows” must transmit or reflect these radiations [1], [14]. In a warm climate, the perfect window transmits visible light while reflecting the near and long infrared wavelengths outside in order to limit overheating [15]. In a cold climate, the ideal window transmits the whole solar spectrum inside (except UV, so 400 nm – 4 μm), but reflects long-wave infrared light (> 4 μm) in order to capture and keep thermal radiation inside the building [15]. At least four key properties are used to assess the performance and characteristics of glazing and windows. These are defined by an international standard (ISO 2003) [8] and are, for example: the heat transfer coefficient (U), visible transmittance (T_V), the Solar Heat Gain Coefficient ($SHGC$) and thermal emissivity (ϵ) [14]. If each coefficient is described in literature, we can observe that T_V is the part of visible light which passes through the glazing material factor for visible light (400-700 nm), and that the U -value ($\text{W}\cdot\text{m}^{-2}\cdot\text{K}^{-1}$) indicates the heat flow from the inside to the outside through the window. [10], [16]. The Solar Heat Gain Coefficient $SHGC$ measures the solar thermal energy transmitted into the building, due to glass transparency of the solar spectrum and the glass solar absorptance. To calculate the $SHGC$ precisely, two types of information are necessary: first, the spectral transmittance and spectral absorptance curves of the glass for the total solar spectrum (280-2500 nm); and second, a solar spectrum, describing the spectral flux density ($\text{W}\cdot\text{m}^{-2}\cdot\text{nm}^{-1}$) for each wavelength.

For decades, both laboratories and industrials have produced many studies treating spectral transmittance and absorptance optical performances of windows. Low-emissivity (low-e) or solar control coatings use several techniques, such as thin layer coatings or electrochromic materials, to shape reflectance and absorptance curves, so as to obtain optimal optical performances for windows. Hundreds of publications which study and propose low-e and solar control coatings for glass are available, depicted their spectral transmittance in Figure 1 [14], [17].

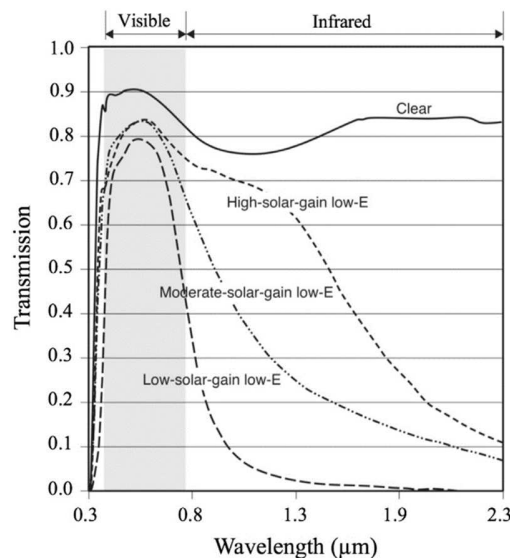


Figure 1: Spectral transmittance curves of different windows with interesting low-e and solar control coatings [14], [17]

Concerning coatings, the second information necessary to calculate the Solar Heat Gain Coefficient *SHGC*, a solar spectrum, has remained unchanged over time. The ASTM G173-03 solar spectrum, proposed in 2003 by C.A. Gueymard, is still used 27 years later [18], [19], especially in many standards, such as the American Society of Testing and Materials (ASTM), the International Organisation for Standardization (ISO) or the International Electrotechnical Commission (IEC) [8], [20–23]. Historically, the atmospheric parameters used to model the ASTM G173-03 solar spectrum are an average value of different clear-sky conditions throughout the USA. Different sites with a Direct Normal Irradiation (DNI) of at least 6 kWh/m² have been considered to propose a unique solar spectrum for the characterization of (Photovoltaic) PV cells in the USA [24], [25]. Just like other examples, the Air Mass value of 1.5 (therefore naming the solar spectrum “solar spectrum AM 1.5”) used in the standard “*was selected based on indications that, for locations ranging from Caribou, ME (latitude 46°52’) to Phoenix, AZ (latitude 33°26’), ~ 50% of solar radiation (...) occurred above or below AM1.5*” [26]. Considering that, the question addressed in this study focuses on the ability of the ASTM G173-03 solar spectrum to characterize low-e and solar control coatings all over the world. We have no doubts about ASTM G173-03, which enables an appropriate characterization of solar performances for smart windows, but it seems essential to point out the small differences when the local atmospheric conditions are taken into account. Studying the validity of the ASTM standard has already been validated in several fields of solar energy, as PV, CPV or thermal collectors [27], [28], [29]. In the case of PV cells, differences have also been pointed out, with or without regard to concentration [27], [28].

2.Theoretical Background

The goal of the study presented in this paper is to evaluate the impact of atmospheric conditions on the solar performances of low-e or solar control coatings. Firstly, we will evaluate the impact of the main atmospheric variables. Secondly, realistic simulations shall be carried out based on local atmospheric data, for 12 sites located around the world, and for a period of at least one year (see Table 1). SMARTS 2.9.8 is used to model Global Tilted Irradiance (GTI) at 37° from a solar spectra based on local atmospheric conditions [19]. The local atmospheric conditions come from the AERONET meteorological database [30], [31]. Finally, we will compare the longtime solar performances obtained with the local atmospheric data to the ASTM G173-03 solar spectrum, currently used as a reference worldwide [8], [32].

2.1. Atmospheric variables

The Earth’s atmospheric composition varies according to space and time, due to a large number of factors such as the seasons, the wind, natural and artificial emissions, the rain, evaporation... etc. [33], [34]. The atmospheric filter, by transforming the space solar spectrum directly emitted by the sun (also called AM0) into the ground-based solar spectrum (often called AM1.5 in the case of the ASTM standard), is not constant everywhere, as shown in Figure 2, due to two atmospheric variables : Aerosol Optical Depth (describing the atmospheric turbidity) and water vapor, as shown in June 2010 [35].

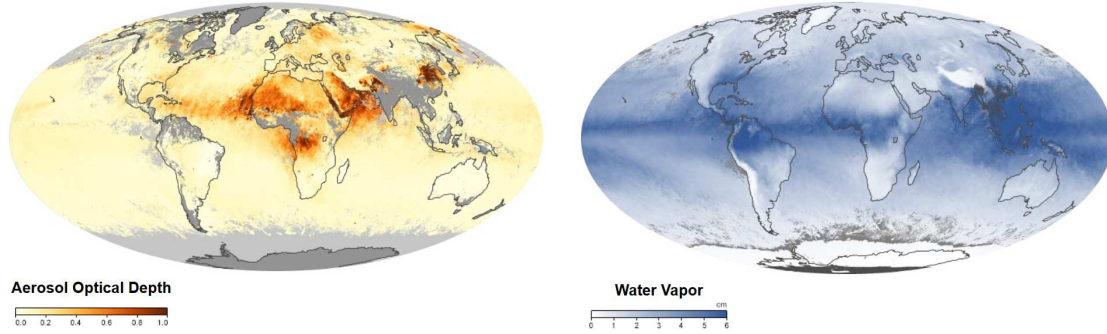


Figure 2 : Left: Aerosol Optical Depth ; Right: Water Vapor in June 2010 [35].

The atmospheric filter is composed of several temporal and local variables. The variables which mostly affect solar spectrum characteristics, and thus the performance of coatings used in the construction industry, are Precipitable Water (PW), Aerosol Optical Depth (AOD), ozone, Air Mass factor (AM), as well as both altitude and atmospheric pressure [32]. The evolution of the particles' size in the aerosol, which impacts the Rayleigh scattering, can be described as an aerosol model or as Angström coefficients (α_1 and α_2) [34]. All the variables can deeply affect the absorption or reflection of sunlight, which transforms the space solar spectrum into the ground solar spectrum. The impact of each atmospheric variable on the solar spectrum is available in literature [28].

2.2.1 Air Mass

The Air Mass (AM) coefficient is defined as the path length ratio (L) of a sunbeam which goes through the atmosphere to reach the surface and the zenith path length (L_0). The AM value is linked to the Solar Zenith Angle (SZA , the angle between the sunrays and the vertical) as shown in the following equation 1 [36].

$$AM = \frac{L}{L_0} = [\cos(SZA) + 0.45665 \cdot SZA^{0.07} (96.4863 - SZA)^{-1.6970}]^{-1} \quad (1)$$

The lowest AM value on Earth is 1.0 ($SZA = 0^\circ$, solar noon at the equator) and the highest is ≈ 7 ($SZA = 82.2^\circ$, when the sun is near the horizon), when the value used in the ASTM G173-03 is 1.5 [18]. Due to Rayleigh scattering, considering the λ^{-4} dependence, the shortest wavelength is more affected by the AM value, with a peak attenuation close to 450 nm [34]. Consequently, a solar spectrum on Earth receiving a high AM value is poorer in visible wavelengths and contains more infrared wavelengths.

2.2.2. Atmospheric turbidity

Aerosol Optical Depth (AOD) quantifies atmospheric turbidity. Turbidity is the relative transparency provided by tiny solid and liquid particles such as pollen, ash, urban haze, or smoke particles suspended in the air, which constitute aerosols. Remember that clouds do not impact Aerosol Optical Depth. Other expressions of AOD such as the Angstrom or Schuepp Turbidity coefficients, or even meteorological range or airport visibility reports are available, but these are not relevant to our study. We set the AOD at 500 nm in our SMARTS calculation because this

data is provided by the AERONET database but also because a similar choice has been made in previous studies [27], [37], [38]. A sole *AOD* measurement, at 500 nm, does not constitute a spectral characterization, especially when compared to the full spectral domain of the solar spectrum (280 – 4000 nm). To describe the optical dependence of aerosol on wavelengths, two methods are available: a standard aerosol model (as in the standard solar spectrum) and two Angström coefficients (α). The Angström coefficient (α) can be a single parameter to describe a large wavelength range, or can be subdivided into sub-indicators. SMARTS uses two sub-indicators (α_1 and α_2) split around 500 nm (380-500 nm and 500-870 nm) to describe a large wavelength range.

2.2.3. Precipitable Water

Precipitable Water (*PW*) describes the atmospheric moisture, that is to say the amount of condensed water (in cm) contained in an atmospheric column, without clouds. As water vapor has an important absorption coefficient in near-infrared zones, this effect cannot be discarded. Precipitable water can vary from ≈ 0 cm (extremely dry, like desert air) to ~ 6 cm (very high humidity level, e.g. tropical air). More details can be found in other publications, especially in the SMARTS user manual [33], [34]. When focusing on the solar spectrum domain (280-2500 nm), the water vapor absorption wavelength band is mostly located in the near-infrared and infrared zones (940, 1,100 and 1,400 nm) [28]. Consequently, a solar spectrum passing through a wet atmosphere is poorer, in terms of flux density, in the infrared region, thus reducing the solar transmittance (defined below) of low-e solar glass.

2.2.4. Ozone column

The ozone column is the amount of ozone (O_3 , in cm) contained in a vertical atmospheric column above any location. Ozone mostly affects the shortest wavelengths, and absorbs the 200-310 nm wavelength range to protect the earth's surface from high UV energy [36], [39].

2.3. Solar spectra modeling: SMARTS

To perform ground-based solar spectra modeling, we used the 2.9.8 version of the Simple Model Atmospheric Radiative Transfer of Sunshine (SMARTS) from January 2019. SMARTS 2.9.8 is a radiative model code, which models the ASTM G173-03 Global Tilt (GT) and the Direct and Circumsolar (DC) solar spectrum used in all the worldwide standards [18], [40]. This new version of SMARTS (2.9.8) has been available since May 2019 [19] and though it provides several improvements, it does not correct important miscalculations. For this reason, we used the new version, and our results could then be compared to the previous studies, which used SMARTS 2.9.5. Succinctly, SMARTS modeling starts from extraterrestrial solar spectra and reduces it, wavelength by wavelength, by calculating the absorption and the reflection provided by the all-important atmospheric phenomenon. To achieve this goal, the SMARTS model needs the parameters listed above. All the details can be found in the literature [33], [34].

To put it simply, SMARTS inputs information from text files and outputs its results into two text files. This model is both user-friendly and efficient but fails to generate a huge quantity of solar spectra. For this study, we coded a script on Scilab (v5.5) [41] in order to read the data.

2.4. Optical and solar performances

Several optical factors need to be calculated so as to have an overview of smart windows and advanced coatings for buildings. These factors are thermal comfort, UV protection and good visibility through the windows. The most important solar radiation glazing factors fall into four categories:

- i. factors describing the ability of UV rays to interact with human skin or materials in the buildings. Ultraviolet solar transmittance (T_{UV}); Solar Material Protection Factor ($SMPF$) and Solar Skin Protection Factor ($SSPF$) are the most common factors [10],
- ii. factors describing the optical behavior within the entire solar spectrum from Ultraviolet to Infrareds (280-2500 nm), such as Solar Transmittance (T_S), Solar Reflectance (R_S) and Solar Absorptance (A_S) [8],
- iii. factors describing visual comfort for the human eye, such as visible solar transmittance (T_{vis}), external or internal visible solar reflectance ($R_{vis,ext}$, $R_{vis,int}$) and color rendering factors (CRF) [23],
- iv. factors describing the thermal behavior of the windows, such a thermal emissivity (ϵ) calculated thanks to the absorptance curves (using Kirchoff's law, emittance equal absorptance at the same wavelength and temperature, $\epsilon(\lambda, T) = \alpha(\lambda, T)$) into the long infrared region (using a black body response) and Solar Factor (SF), calculated from T_S , R_S and ϵ .

This section focuses on the differences, in terms of optical performances, between solar spectra from local atmospheric data and the ASTM G173-03 solar spectrum (AM 1.5), which is most generally used. In conclusion, only the factors requiring a full solar spectrum (280-2500 nm) are relevant. For this reason, our work focuses on solar transmittance (T_S) and solar absorptance (A_S). In this paper, we use data found in other studies, using real samples with the same thickness. Please note that solar reflectance (R_S) can be deduced thanks to the law of conservation of energy, if necessary. If the UV flux is also a function of the local weather, the factors described in section i), T_{UV} , $SMPF$ and $SSPF$ are not calculated, to avoid adding unnecessary information to our study. The factors describing visible comfort for the human eye in section iii), are not taken into account either, since no solar spectrum is required [8]. Also, the Solar Factor in section iv) is not included, because thermal emittance (ϵ) is needed, which requires absorptance curves for the total infrared region which are not measured for glass.

Solar transmittance (T_S), and solar absorptance (A_S), are the ability for a sample to transmit (T) and absorb (A) the solar flux density over the total solar wavelength range. Both values will thus be a number between 0 and 1, calculated in the UV, visible and infrared region of the solar spectrum, i.e. 280-2500 nm [8], [22]. The law of conservation of energy is ensured by the three solar performances: solar transmittance, added to both solar absorptance and solar reflectance, is always equal to one.

$$A_S = 1 - T_S - R_S \quad (2)$$

To calculate solar transmittance (T_S) or solar absorptance (A_S), the spectral transmittance $T(\lambda)$ or absorptance $A(\lambda)$ of each sample is linked to the intensity of a solar spectrum $S_n(\lambda)$ in

$\text{W}\cdot\text{m}^{-2}\cdot\text{nm}^{-1}$, in the whole solar region, from 280 to 2500 nm. The irradiance chosen is Global Tilted Irradiance (GTI) and not Direct and Circumsolar (DC), chosen based on our applications (buildings and windows). It is defined as a 5 nm step, according to the standard recommendations [22].

$$T_s = \frac{\int_{280}^{2500} T(\lambda) \cdot S_n(\lambda) \cdot d\lambda}{\int_{280}^{2500} S_n(\lambda) \cdot d\lambda} \quad (3-a)$$

$$A_s = \frac{\int_{280}^{2500} A(\lambda) \cdot S_n(\lambda) \cdot d\lambda}{\int_{280}^{2500} S_n(\lambda) \cdot d\lambda} \quad (3-b)$$

We observed that the solar region (280-4000 nm) is different from the solar performance calculation (280-2500 nm). The first reason is metrological: access to the sample's optical performances from 2500 to 4000 nm is not easy. In the near IR region, the irradiated power is so scarce that the overall weight of the 2500-4000 nm region is only 0.0018 of the total solar spectrum. The second reason is comparative : the actual standards [20] recommend using an ASTM G173-03 solar spectrum from 280 to 2500 nm. As all the values are discrete, the integration is solved thanks to a summation ($d\lambda$ is replaced by $\Delta\lambda$).

2.5. Sample presentation

Seven samples of coated glass used in buildings are studied in this paper. For all the samples, spectral transmittance and spectral absorptance values are necessary throughout the solar spectrum (280-2500 nm). Figure 3 and Figure 4 both show the transmittance and absorptance of the samples. All the samples have the same thickness (1mm). There are two kinds of samples: two samples were obtained by modeling (named "Glass without coating" and "Standard AR glass") and five samples were used from studies. We performed the modeling, using a transfer matrix method described in our previous papers [42]. The first sample (black dotted line), used here as a reference, is a 1 mm BK7 glass, without any coating. An uncoated glass has a close to 1.5 refractive index, therefore a glass surface without antireflective coating shows a standard reflectance of 5% per face in all the solar spectrum [42]. The second sample (black dash line) is a commercial triple layer AR coating, [43]. This coating shows high transmittance on the visible spectrum with a peak at 400 nm. The transmittance decreases in the near infrared region to reach 70-80% transparency in the infrared region. Both of these samples show a very low percentage of absorptance (Figure 4). Their transmittance and absorptance curves were obtained by modeling [42]. The five other samples are low-emissivity glass (low-e) or solar-control coatings used in smart windows. The curves were obtained by digitalization or directly from the authors of previous studies focusing on smart windows or low-e coatings [44–48]. These types of glass are designed for highly visible light transmittance, with low or high reflectance in the infrared region, depending on climate conditions, as explained above. Today, a large number of different coatings have been designed to ensure low-e glazing, the materials frequently used are typically doped metal oxides and metal films sandwiched between dielectric layers [1]. The green curve shows a low-e glass for cold climates designed to maximize solar flux (high solar gain). Three different samples, shown with blue curves (from 1 to 3) have coatings designed for moderate

solar gain. All of the blue samples show highly visible transmittance and different shapes, due to the coating's composition which impacts both transmittance and absorptance in the near and long infrared regions. The last sample, the red curve, shows low solar gain, due to moderate visible transmittance and extremely low transmittance in the infrared spectrum ($\lambda > 1000$ nm). Using the law of conservation of energy, it is possible to deduce the reflectance behaviour of each sample. If the high solar gain sample shows high reflectance in the infrared region to reflect the thermal radiation outside the building, thermal emittance (ϵ) for the low solar gain must be around 40%.

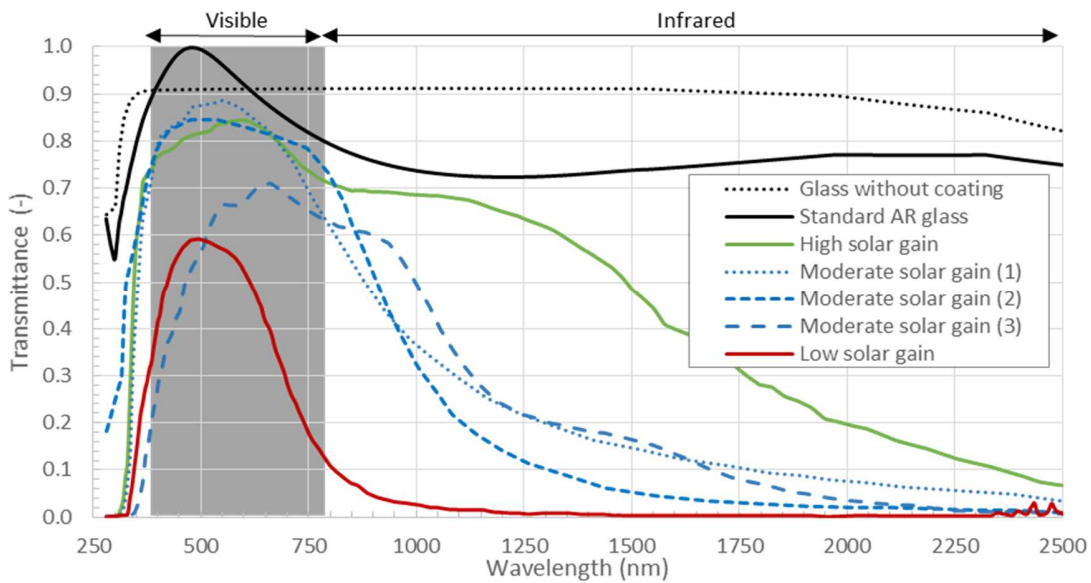


Figure 3: Spectral transmittance curves for low-e samples

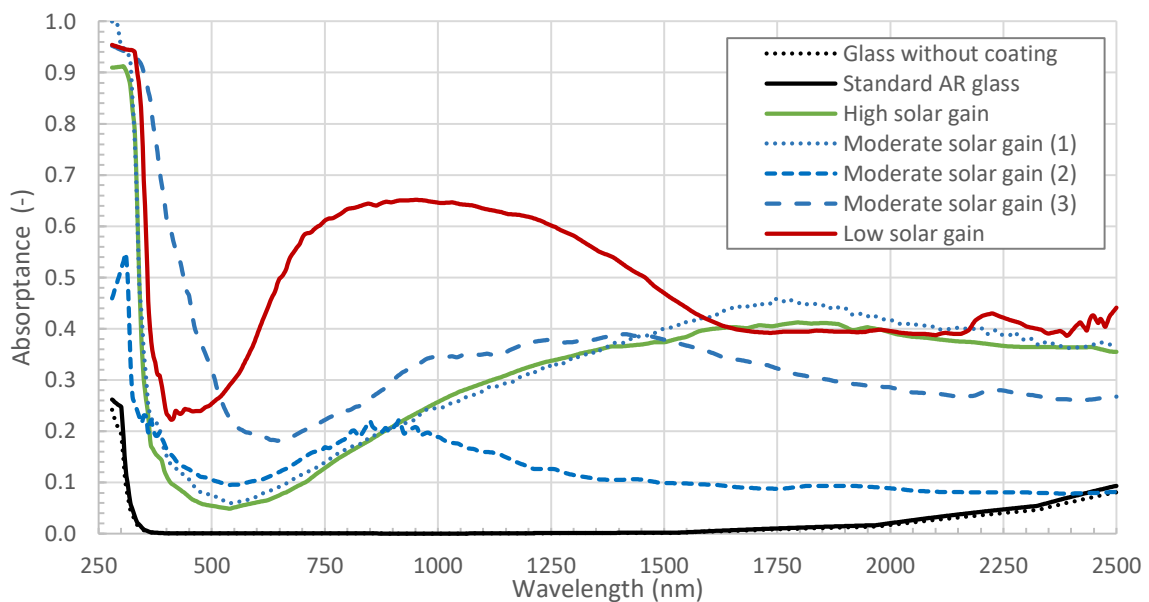


Figure 4: Spectral absorptance curves for low-e samples

3. EFFECT OF ATMOSPHERIC VARIABLES ON LOW-E GLASS

Figures 5, 6 and 7 demonstrate the impact of the three main atmospheric variables (Air Mass, Aerosol Optical Depth and Precipitable Water) on low-e glass solar transmittance and absorptance. One may expect that these changes in spectral distribution of the solar spectrum would have potential effects on solar performance. In order to validate this theory, the atmospheric variables were studied one by one, setting other variables at their reference value used to model the ASTM G173-03 solar spectra ($AM = 1.5$, $AOD = 0.084$ and $PW = 1.416$ cm). Graphs indicating the impact of the variables (AM, PW, AOD) on the solar spectrum are detailed in other previous literature [28].

3.1. Air Mass Impact

Air Mass (AM) is defined as atmospheric thickness related to the shortest path ($AM = 1$, solar noon at the equator). AM is generally the most sensitive variable of the solar spectrum. Figure 5-a shows the effects of low-e glass on solar transmittance by varying AM , in percentage points (pp). We have observed, on all the glass types studied, that the higher the AM factor, the more the glass transmits solar energy. For example, with an AM factor superior to 3, (location with a high latitude or during the first or last hour of the day), solar transmittance can increase by several percentage points. The only exception is the “Moderate solar gain (2)” sample. As shown in Figure 3, the transmittance of this sample quickly decreases in the near-infrared range, showing a poor ability for this glass to transmit sunlight with high AM . In other words, AM increases the relative importance of the longest wavelengths, and glass which is relatively more transmitting in the longest wavelengths would be beneficially affected by an increased air-mass factor.

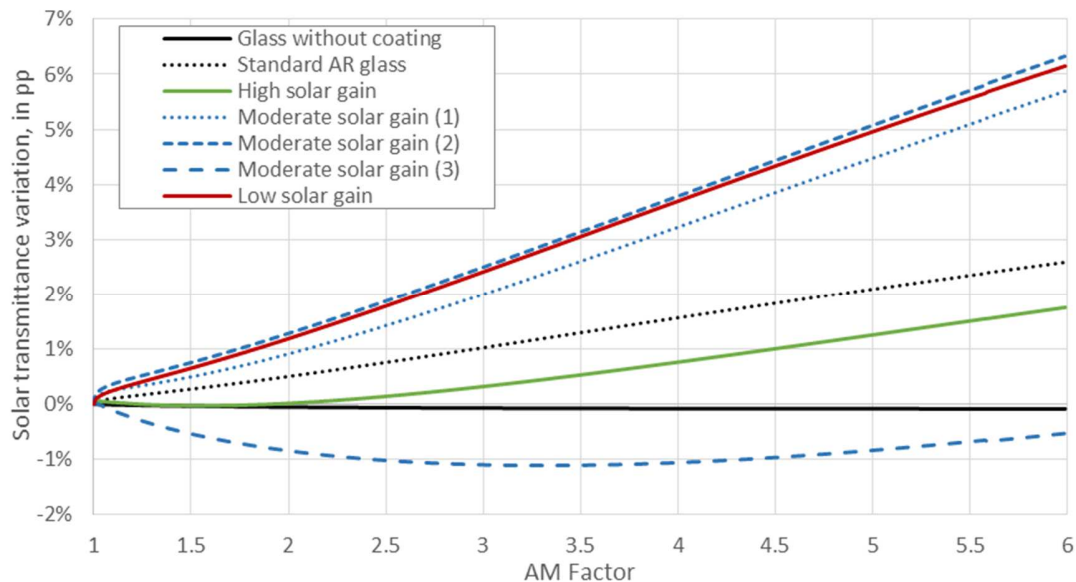


Figure 5-a: Low-e glass solar transmittance depending on the AM factor

Contrary to solar transmittance, the solar absorptance of most low-e glass (see Figure 5-b) decreases with high AM , except the “Moderate solar gain (2)” sample. High solar gain glass and low solar gain glass show the most important decreases in solar absorptance. The “Moderate solar gain (2)” sample demonstrates the law of conservation of energy: the solar absorptance increases while the solar transmittance decreases.

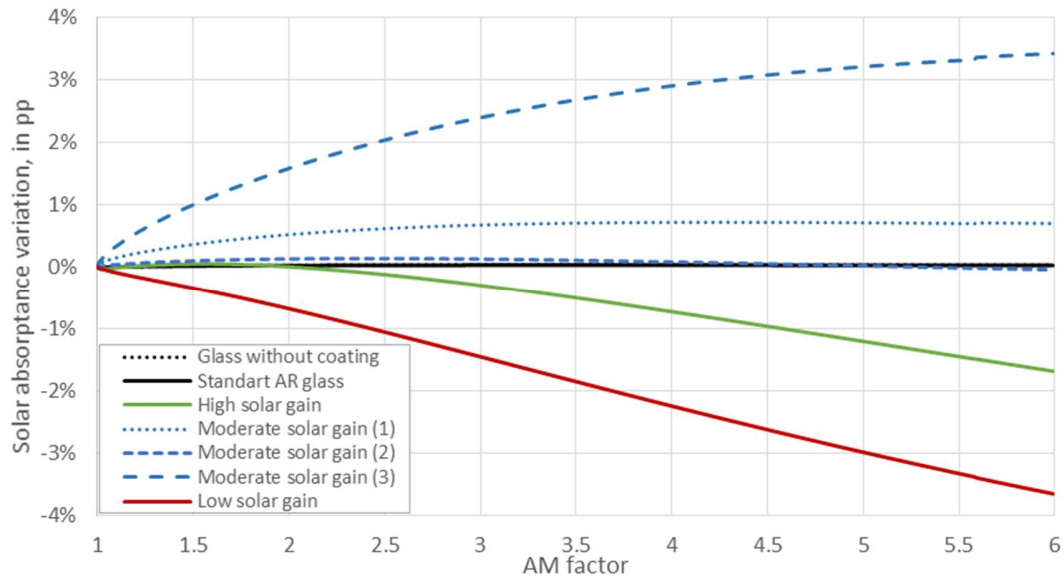


Figure 5-b: Solar absorptance of low-e glass depending on the AM factor

3.2. Impact of Precipitable Water

Precipitable Water, or the quantity of water in an atmospheric column, has an impact on the solar spectrum in specific absorption ranges only, contrary to AM and AOD , which both affect the whole solar spectrum.

Figure 6-a describes, in percentage points (pp), the solar transmittance losses of our samples. All coated samples are impacted. The solar transmittance loss is proportional to the precipitable water quantity, and varies from one sample to another. A standard atmosphere is used for comparison ($PW = 1.416$, represented by a black vertical line). A drier atmosphere increases the solar transmittance of coated glass. Conversely, a tropical atmosphere ($PW > 4$ cm) decreases solar transmittance by 1 to 2 percentage points, depending on the sample and the PW value. The low-e glass samples with a narrow transmission range (like “Moderate solar gain (1) and (2)” or “low solar gain”, see Figure 3) are more impacted.

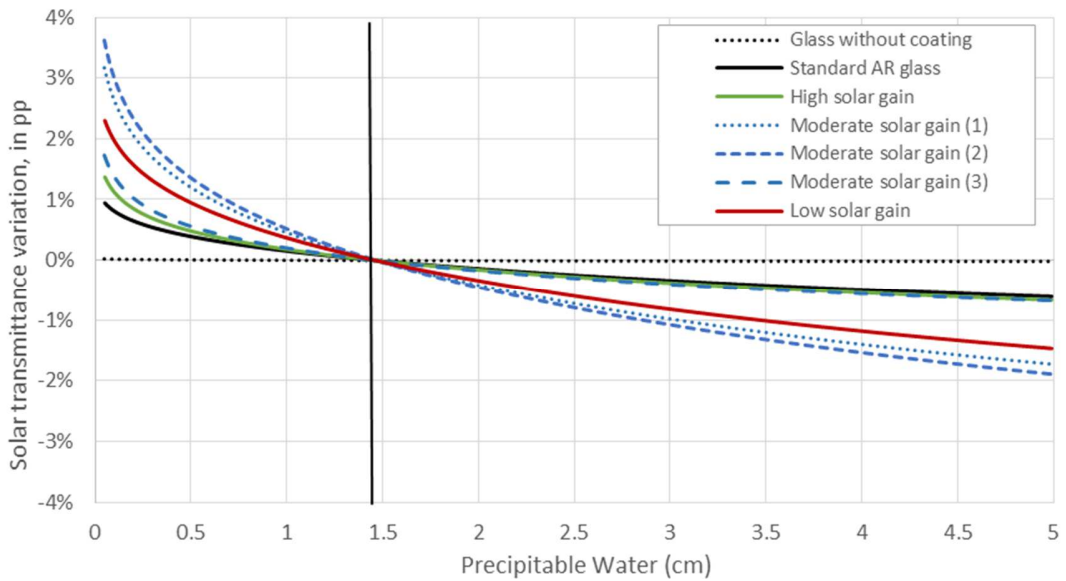


Figure 6-a: Solar transmittance of low-e glass depending on Precipitable Water

A solar spectrum with a drier or wetter atmosphere, compared to standard one, also has an impact on solar absorptance. Among the glass samples studied, the two most impacted are the low solar and the high solar gain samples: The first one has an absorptance peak in the near infrared region, and the second shows a constant and growing absorptance (see Figure 4). In any case, the solar absorptance variation, between extremely dry and extremely wet atmospheres, is around +/- 1%, which is relevant, without being problematic.

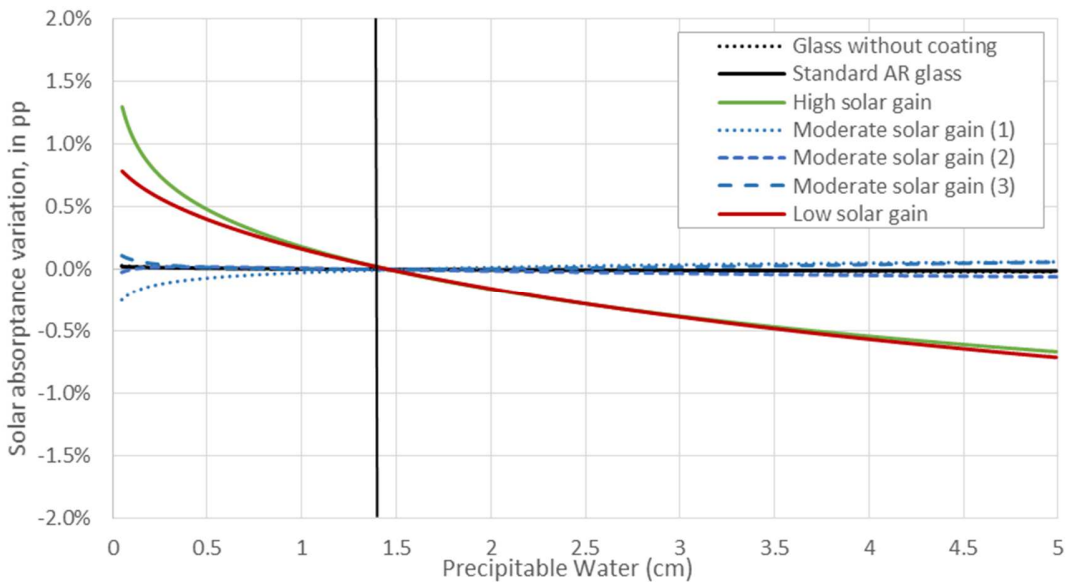


Figure 6-b: Solar absorptance of low-e glass depending on Precipitable Water

3.3. Impact of Aerosol Optical Depth

As previously described, Aerosol Optical Depth (*AOD*) is related to the amount of solar radiation attenuated due to atmospheric aerosols made up of fine particles, urban haze, sea salt, desert dust or smoke particles. Considering the typical *AOD* wavelength dependence, the solar spectrum attenuation mainly occurs at short wavelengths (300-1000 nm). The *AOD* value measured at 500 nm for the standard solar spectrum can vary from almost 0 (an ideally clean atmosphere) to 1 (an atmosphere with high turbidity). Specific and rare events, like dust storms, forest fires or volcanic eruptions, due to which the *AOD* value can rise up to 3.0, are not considered in this paper. The distribution of the particles in the aerosol, according to their size, is directly dependent on the location of the aerosol. It can be characterized by an aerosol model or by the Angström coefficients (α_1 and α_2) distributed from either side of the *AOD* (see section 2.2.2.) In the case of the standard ASTM G173-03 reference spectrum, the Shettle & Fenn Rural reference aerosol model is used with $AOD_{500nm} = 0.084$. Figure 7-a describes the solar transmittance of low-e or solar control glass according to *AOD* values. A similar conclusion to *AM*'s effect can be drawn. Solar transmittance variation grows with aerosol optical depth, as near-infrared and infrared wavelengths are less reflected or absorbed by the aerosol. As the *AOD* effect on the solar spectrum is more complex than *AM*, the increase is not strictly linear, as observed with *AOD* values near 0.2.

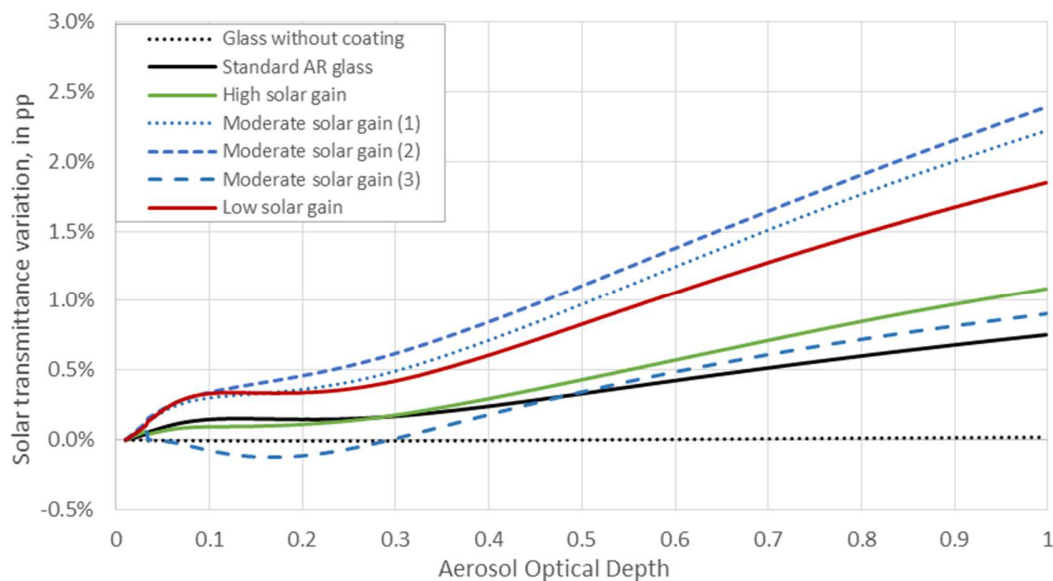


Figure 7-a: Solar transmittance of low-e glass depending on the *AOD* value

Solar absorptance variation according to the *AOD* (Figure 7-b) has a similar shape as *AM*, albeit with lower values. “Moderate solar gain” samples (from 1 to 3) increase their absorptance values, but never beyond the 0.5 percentage point. Low and high solar gain low-e glass absorbs less solar radiation as the *AOD* increases. Finally, and as expected, the solar absorptances of glass without coating and of standard glass are not affected by the *AOD*. This is to be expected because the transmittance of this glass is relatively constant over the full solar spectrum wavelength range.

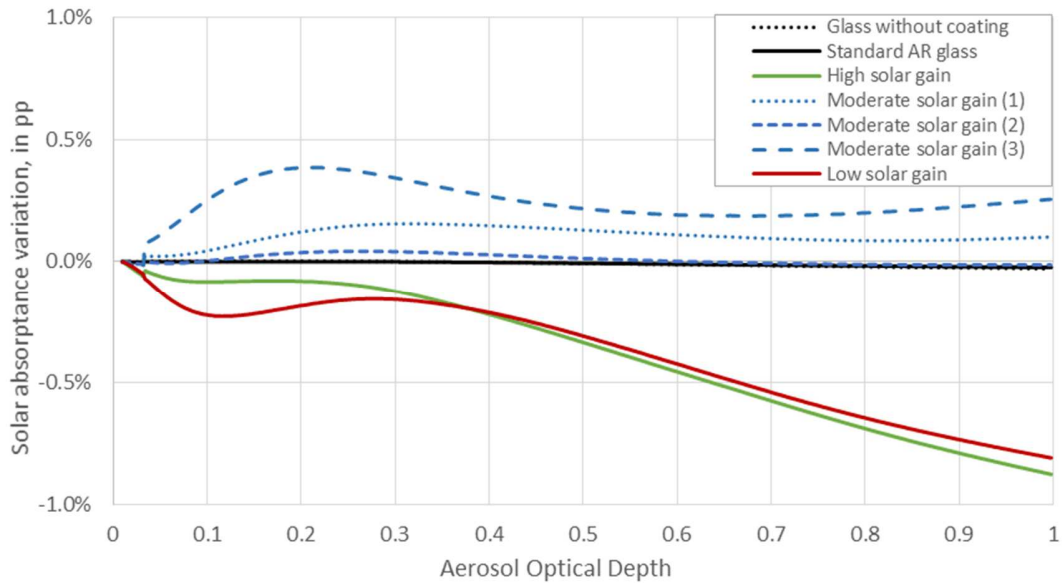


Figure 7-b : Solar Absorbance of low-e glass depending on the AOD value

3.4. Summary

The variation of the solar optical performances of low-e or solar control glass, depending on the three main atmospheric variables (AM , PW and AOD), greatly depends on the glass sample. Graphs indicating the impact of AM , PW , AOD on the spectrum are available thanks to A.Voissier [28]. As expected, AM has the most impact on optical performances (T_s , A_s , etc). We observed that as AM and turbidity coefficients increase, so does solar transmittance, thus reducing the short wavelength in the solar spectrum. On the contrary, a moist atmosphere reduces solar transmittance while a drier atmosphere has the opposite effect. Solar absorbance can be increased up to 3% (percentage point) by a high AM factor (>4 represents a low solar zenith angle). The two other atmospheric variables (PW and AOD) have less impact on solar absorbance. The impact of atmospheric variables has already been pointed out for PV cells and CPV cells in [27], [28], [29].

4. LONGTIME SOLAR PERFORMANCES FOR 12 SITES LOCATED AROUND THE WORLD

To complement the results obtained previously, in this section we will discuss the real tests that were performed using long-term atmospheric variables (AM , AOD , PW). Indeed, these parameters evolve simultaneously, hour after hour, depending on the weather, the seasons or specific events. The impact of the local weather on the optical performance of low-e glass was studied at 12 different locations situated around the world, each with different atmospheric conditions. For each site, we modelled the solar spectra as much as possible for at least a year, using real atmospheric variables before calculating the solar optical performances of low-e glass. All the values obtained were compared to the ASTM G173-03 standard, the solar spectrum reference.

4.1. AERONET Database and modelling

To obtain the atmospheric variables of different sites, we used AERONET. AERONET, which stands for AErosol ROBotic NETwork, is a free and public database which provides data from atmospheric conditions all around the world. This ground-based remote sensing aerosol network was established by NASA and PHOTON [30]. Its website is available at : <https://aeronet.gsfc.nasa.gov> [31]. The AERONET federation has imposed the standardization of instruments, calibration and processing and provided researchers with high-quality data for decades. In November 2020, over one thousand stations were available worldwide. We only used the 2.0 quality assurance data, which is the highest level available after cloud screening, calibration, and degradation correction. All the atmospheric parameters previously described, such as *AOD*, *PW*, Angström coefficients (α_1 and α_2), ozone layer and solar zenith angle were available. This allowed us to model solar spectra with SMARTS without using other data [34].

Even if several preconfigured atmospheric models are available in SMARTS, we used the two Angström coefficients (α_1 and α_2), also provided by AERONET, to model the aerosol. This way, SMARTS could estimate the size distribution of the particles. Global Tilted Irradiance (GTI) solar spectra are calculated thanks to the SMARTS radiative model [12]. Even if the *AM* values can be calculated directly from the solar zenith angle (*SZA*, *equ.* (1)), we used the value proposed in the AERONET database.

4.2. Selected Locations

Twelve different locations were selected according to the following criteria:

1. They should provide level 2.0 quality data (the highest quality provided by AERONET) for several years, without important discontinuity. This first criterion was the most difficult to meet, and most of the locations proposed in AERONET do not meet this criterion [49], [28], [50].
2. They must represent the different weather conditions found around the world as closely as possible.
3. Specific atmospheric conditions must be represented if possible, for example: sites with low and high ozone, *PW* or *AOD*.

In related bibliography, W. Jessen et al. [27] used 5 sites in their study about thermal solar materials, while Vossier et al. [26] used 6 sites in their study on CPV solar cells [28]. In addition, our solar spectra data bank was used to calculate the longtime solar performances of smart windows. The necessity of low-e or solar control glass was not considered in the selection of the locations. A selected site could be chosen for several reasons, such as geographical interest (high altitude, high or low latitude), specific atmospheric conditions (low or high *PW*, *AOD*... etc.) or specific location (large cities, near the ocean). Table 1 presents the different sites according to their name in the AERONET software and their location (latitude and longitude). As our aim was to analyse a complete year without an important discontinuous period, the simulated years (not specified in the table) could be different for each location but do not have any impact on the overall conclusion. GHI (Global Horizontal Irradiance, in kWh/m²/y) was given as complementary information, from the SolarGis interactive web map [51]. The selected locations cover a large part of the latitude and longitude of the Earth, with stations on both sides of the

equator. Figure 8 shows the selected locations on a GHI (Global Horizontal Irradiation, kWh/m²) world solar map. As for geographical distribution, five sites are located in the Northern hemisphere, three in the Southern hemisphere and four near the equator. One site (Casleo n°2) is situated at high altitude (up to 2,000 m), in the Argentinian desert. The city of Helsinki was added because it is the northernmost station in the AERONET database (latitude: 60.204°). Likewise, Singapore is an interesting site for a dual reason: it is situated near the equator (1.298°) while having tropical weather (see Table 2). Dakar (n°4), La Parguera (n°7) and American Samoa (n°10) are close to the equator and located near the ocean. Birdsville (n°2) is a unique site located in the middle of the Australian desert. Casleo (n°3) and Mezaira (n°8 near Abu Dhabi), present the most abundant solar resource in the world, with GHI up to 2400 kWh/m²/y. For each sites, we selected atmospheric data for five years. The years selected years are between 2015 and 2020, when possible. Two sites are exceptions: Casleo and Birdsville where coverage over this periode is not available, probably due to the shutdown of the station. As far as possible and according to the data available, this five-years has been respected.

Table 1: Selected locations

N°	Location name (in Aeronet)	Country (-)	Latitude (°)	Longitude (°)	GHI (kWh/m ² /y)	Altitude (m)	Years
1	Beijing	China	39.977	116.381	1348	92	2015-2020
2	Birdsville	Australia	-25.899	139.346	2490	46.5	2013-2018
3	Casleo	Argentina	-31.799	-69.296	2676	2485	2011-2014
4	Dakar	Senegal	14.394	-16.959	2113	21	2015-2020
5	Helsinki	Finland	60.204	24.961	1000	52.8	2015-2020
6	Neon Wood	USA	47.128	-99.241	1430	590	2015-2020
7	La Parguera	Puerto Rico	17.970	-67.045	2126	12.4	2015-2020
8	Mezaira	AEU	23.105	53.755	2440	201	2014-2019
9	Palaiseau	France	48.712	2.215	1156	156	2015-2020
10	American Samoa	American Samoa	-14.247	-170.564	1815	76	2015-2020
11	Seoul	South Korea	37.458	126.951	1438	116	2015-2020
12	Singapore	Singapore	1.298	103.780	1681	30	2015-2020

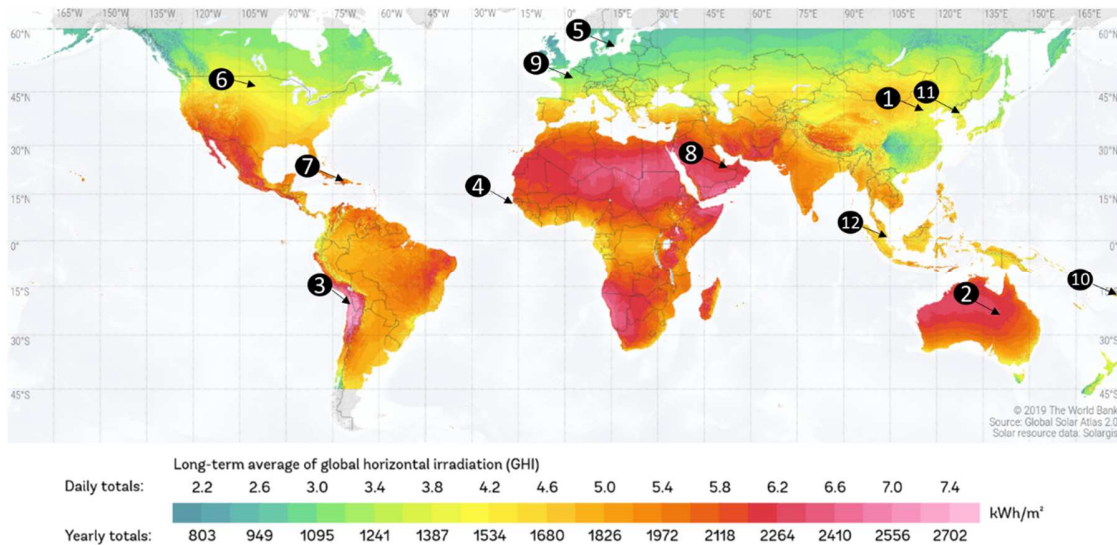


Figure 8. Selected locations on a Global Horizontal Irradiation world solar map [52]

Table 2 presents the atmospheric parameters of values such as turbidity (AOD), precipitable water (PW) etc. for each selected location. With geographical location, atmospheric conditions are the second criterion selected. A site can be chosen for specific atmospheric conditions despite a less interesting geographical situation. As previously mentioned, the values presented are time-weighted. Weighted values are necessary because the AERONET database is rich in points close to the sunrise or sunset, which are not representative of the conditions expected in the daytime. Atmospheric conditions used to model the ASTM reference solar spectrum are given as a reference by literature [18].

Most sites, except Birdsville, Casleo, Helsinki and American Samoa, have a higher AOD than the ASTM G173 ($AOD = 0.084$). The AOD variation can be important, as in Mezaira located in the UAE desert (four times the ASTM G173 AOD value), in Dakar, or in Beijing or Seoul, two megalopolises. In comparison, Casleo is situated at a high altitude (2,485 m) and has the purest atmosphere ($AOD = 0.025$). The two Angström coefficients (α_1 and α_2) which describe the aerosol model are all quite different, showing location's aerosol variability. As for Precipitable Water, the distribution is quite equitable: 4 sites have a drier atmosphere than the reference values ($PW < 1.416$ cm), 4 sites are close to the reference values (Birdsville, Neon Wood, Mezaira, Palaiseau) and the last 4 sites have a moist atmosphere, typical of tropical locations. We noticed that the sites with the driest atmosphere also have the highest altitude (Casleo, n°3). On the contrary, the tropical locations (Dakar, La Parguera, American Samoa and Singapore), with low latitudes and located near an ocean, have the moistest atmospheres recorded. The record value is observed for Singapore, with a PW value of 4.781 cm. The ozone (O_3) layer, a gas which can absorb UV rays, is given here in cm. For all of the sites, the total ozone column is lower than the one used for the ASTM G173-03 DC, except for Beijing and Helsinki. The tropical sites (Dakar, La Parguera, American Samoa, Singapore), and the high altitude site (Casleo, 2485 m) have the lowest ozone layer values. If we can expect more or less UV flux intensity in the local solar spectra, we can recall that: i) atmospheric thickness (AM factor) must be considered and ii) other gases and atmospheric parameters (PW , AOD) impact the UV light reaching the ground.

The AM factor is given for information only, and calculated from the solar zenith angle for one year. The given measurements are not perfectly, nor equally distributed during the year, thus the AM value can be overestimated or underestimated. Despite this, correlation between latitude and the AM value is correct. Two sites, Beijing and Seoul, show a specific combination of high AOD and AM value.

Table 2: Longtime mean atmospheric values for the different locations

N°	Location name (in Aeronet)	Latitude (°)	AOD at 500 nm	PW (cm)	α_1 (-)	α_2 (-)	AM	Ozone (cm)
	ASTM G173-03		0.084	1.416			1.5	0.343
1	Beijing	39.977	0.596	1.328	1.016	1.063	2.072	0.338
2	Birdsville	-25.899	0.047	1.639	1.395	0.764	1.882	0.274
3	Casleo	-31.799	0.025	0.438	1.012	0.501	1.912	0.275
4	Dakar	14.394	0.397	2.563	0.415	0.333	1.736	0.271
5	Helsinki	60.204	0.077	1.087	1.321	1.310	2.614	0.346
6	Neon Wood	47.128	0.103	1.550	1.361	1.364	2.238	0.327
7	La Parguera	17.97	0.158	3.647	0.622	0.329	1.770	0.268
8	Mezaira	23.105	0.369	1.884	0.842	0.563	1.817	0.274
9	Palaiseau	48.712	0.155	1.679	1.168	1.209	2.277	0.337
10	American Samoa	-14.247	0.056	4.058	0.696	0.527	1.748	0.255
11	Seoul	37.458	0.430	1.402	1.154	1.330	2.070	0.336
12	Singapore	1.298	0.410	4.781	1.274	1.389	1.702	0.264

4.3. Longtime optical performances

The complete collection of thousands of solar spectra per site allows us to calculate the longtime solar performance of each sample, noted $A_{s,lt}$ for the solar absorptance, and $T_{s,lt}$ for the solar transmittance. Then, similarly to solar transmittance (T_s) or solar absorptance (A_s), we defined the ratio of the total transmitted or absorbed energy, divided by the total energy available for several years, [8], [22]. As the solar spectrum changes over time, we added the subscript (n) so as to point out that two solar performances can be different, depending on their solar spectrum. Since the difference in time between two measurements in the AERONET database is not fixed, we calculated the time gap Δt_n , between a given solar spectrum (n) and the following one ($n+1$). Both a minor time difference of less than 15 minutes, and a larger one superior to several hours, are excluded, in order to avoid miscalculation [53].

$$A_{s,lt} = \frac{\sum_{n=1} S_n \cdot A_{s,n} \cdot \Delta t_n}{\sum_{n=1} S_n \cdot \Delta t_n} \quad (3-a)$$

$$T_{s,lt} = \frac{\sum_{n=1} S_n \cdot T_{s,n} \cdot \Delta t_n}{\sum_{n=1} S_n \cdot \Delta t_n} \quad (3-b)$$

It should be noted that the longtime irradiance ($I_n \cdot \Delta t_n$) calculated thanks to this method, cannot substitute for the annual irradiance (GTI in our case) found in a database. The values

given here are only for 4 to 5 years, while sites like SolarGis provide average solar potential values calculated for many years [51].

5. RESULTS

The results first consist in the computation of the longtime solar transmittance and absorptance, and then their comparison with the values calculated with the standard reference, the ASTM G173-03 Global Tilt solar spectrum [8], [18]. Our solar spectra databank is used to calculate the longtime solar performances.

5.1. Longtime Solar Transmittance

The longtime solar transmittance of low-e glass corresponds to the total quantity of the sun's radiant energy which passes through a window in a year. Table 3 shows the results, with the lowest values in red and the highest values in green. To start, an uncoated glass showed a very constant solar transmittance, with longtime values from the different sites near the ASTM value. If a standard antireflective coating is applied, the typical longtime solar transmittance is between 82.7% and 85%. Sites at a low altitude, as well as low AM and high Precipitable Water values (La Parguera and American Samoa) show values superior to the ASTM standard. For these sites, the ASTM solar spectrum underestimates solar transmittance, especially for low solar gain (≈ 1 of a percentage point). For the others, except Beijing and Seoul, the longtime values calculated with the standard solar spectra are near the longtime values. As for Beijing and Seoul, they are the only exceptions in the table, showing specific behaviors. The calculated longtime solar transmittance for these two sites is the lowest of all the glass samples. For the "low solar gain" and "moderate solar gain (1) and (2)" samples, the difference in solar transmittance goes up to 5 percentage points (pp). For these two sites, the use of the ASTM resulted in a highly exaggerated overestimation of the real solar transmittance, and, as a consequence, the solar gain provided by the windows. Fortunately, the use of high solar gain windows was suggested at these sites, and the result is that the ASTM overestimation is only two percentage points. This specific behavior is due to the combination of two factors: high *AOD* (0.598 for Beijing and 0.437 for Seoul) and high *AM* values (2.09 for Beijing and 2.04 for Seoul). As Figure 5 and Figure 7 show, these two factors reduce solar transmittance. The specific combination of these two factors strongly impacts the solar spectrum, which leads to a decrease in solar transmittance. Different sites show that the combination of different factors reduces solar transmittance, as illustrated by Helsinki ($AM = 2.61$; $AOD = 0.077$), Dakar ($AM = 1.75$; $AOD = 0.397$) or Mezaira ($AM = 1.82$; $AOD = 0.370$).

Table 3: Longtime solar transmittance of low-e glass for 12 different atmospheric conditions

	Glass without coating	Standard AR glass	High solar gain	Moderate solar gain (1)	Moderate solar gain (2)	Moderate solar gain (3)	Low solar gain
ASTM	90.6%	84.3%	70.4%	59.9%	59.3%	48.6%	26.5%
Beijing	90.5%	82.7%	68.1%	54.9%	53.6%	46.5%	22.5%
Birdsville	90.6%	83.9%	70.1%	59.0%	58.2%	48.6%	25.6%
Casleo	90.5%	83.9%	69.8%	58.5%	57.6%	47.7%	25.5%
Dakar	90.5%	84.4%	70.3%	60.0%	59.3%	48.4%	26.7%

Helsinki	90.6%	83.7%	69.6%	58.0%	57.0%	47.8%	25.0%
Neon Wood	90.6%	84.1%	70.1%	59.2%	58.5%	48.3%	26.0%
La Parguera	90.5%	84.9%	70.8%	61.3%	60.8%	48.9%	27.8%
Mezaira	90.5%	83.9%	69.8%	58.7%	57.9%	48.1%	25.6%
Palaiseau	90.5%	83.9%	69.7%	58.5%	57.7%	48.0%	25.5%
American Samoa	90.6%	84.8%	70.8%	61.2%	60.8%	49.1%	27.9%
Seoul	90.5%	82.9%	68.6%	55.8%	54.6%	47.2%	23.0%
Singapore	90.5%	85.0%	70.9%	61.6%	61.1%	49.0%	28.1%

5.2. Longtime Solar Absorptance

As previously discussed, the longtime solar absorptance corresponds to the total quantity of the sun's radiant energy absorbed by the glass and the coating. Table 4 shows the solar absorptance results, with the lowest values in green and the highest values in red. The data relating to several low-e glass samples show a greater homogeneity: the difference in percentage points between sites or when compared to the ASTM references, is minimal. We can thus conclude that the ASTM solar spectrum can correctly predict the solar absorbed flux. The difference between the lowest value (in green) and the highest (in red) is often only a few digits. For all the samples, except for the "High solar gain" and "Low solar gain", the maximum difference between the sites is inferior to 1.2 percentage point. Indeed, solar absorptance values are often lower on (regular / basic / untreated) glass, as windows are not specifically made to absorb solar flux. Consequently, the variations due to local atmospheric conditions are lower. According to the ASTM values, Beijing and Seoul (two sites with high *AOD* and *AM* values) have the maximum deviation, contrary to the longtime solar transmittance. It is interesting to observe that, for the low solar gain and the high solar gain samples, these two sites have the highest value (49.3 % and 49.2%), showing their ability to absorb the sunlight and to convert it into heat. Likewise, tropical sites like La Parguera and Singapore have the lowest longtime solar absorptance value for the "high solar gain" and "low solar gain" samples. The "moderate solar gain 3" sample shows a maximum difference between the sites of 1.2 percentage point, between Seoul and Singapore. In this case, tropical sites (La Parguera and Singapore) have highest absorptance values. This behavior is due to a high spectral absorptance of the "moderate solar gain 3" sample in UV (greater than 0.5 or 50% below 400 nm) as can be seen in Figure 4.

Table 4: Longtime solar absorptance of low-e glass for 12 different atmospheric conditions

	Glass without coating	Standard AR glass	High solar gain	Moderate solar gain (1)	Moderate solar gain (2)	Moderate solar gain (3)	Low solar gain
ASTM	0.3%	0.2%	17.5%	12.3%	14.2%	32.0%	47.7%
Beijing	0.3%	0.3%	19.4%	11.8%	14.1%	31.3%	49.3%
Birdsville	0.3%	0.2%	17.8%	12.2%	14.2%	31.5%	48.3%
Casleo	0.3%	0.2%	18.1%	12.2%	14.2%	32.1%	48.1%
Dakar	0.3%	0.2%	17.5%	12.3%	14.1%	32.1%	47.5%
Helsinki	0.3%	0.2%	18.2%	12.0%	14.1%	31.7%	48.3%
Neon Wood	0.3%	0.2%	17.8%	12.2%	14.2%	31.8%	47.9%
La Parguera	0.3%	0.2%	17.1%	12.4%	14.1%	32.2%	47.0%
Mezaira	0.3%	0.2%	18.0%	12.1%	14.1%	31.6%	48.0%
Palaiseau	0.3%	0.2%	18.0%	12.1%	14.1%	31.6%	48.1%

American Samoa	0.3%	0.2%	18.0%	12.1%	14.1%	32.0%	47.3%
Seoul	0.3%	0.3%	19.1%	11.9%	14.1%	31.1%	49.2%
Singapore	0.3%	0.2%	17.0%	12.4%	14.1%	32.3%	46.9%

DISCUSSION & CONCLUSION

With the growing concern of energy consumption in the construction industry, it has become crucial to understand the role of solar flux. The use of low-e and solar control glass in buildings plays an important energy-saving role. In order to increase our understanding of the Solar Heat Gain Coefficient, in this paper we endeavoured to calculate the solar transmittance and absorptance of a panel of low-e glass samples in correlation with local atmospheric variables, as opposed to using the default calculations of the ASTM G173-03 solar spectrum. We have shown that the Air-Mass factor, Aerosol Optical Depth and Precipitable Water play an important part and can modify solar flux, whether it is transmitted or absorbed by smart windows. Using 12 locations, we performed realistic modelling to calculate the longtime solar transmittance and absorptance using a databank of thousands of solar spectrum models according to local atmospheric conditions. This modelling was performed thanks to the AERONET database, using SMARTS software. We have demonstrated that in specific conditions, such as high Air-Mass and Aerosol Optical Depth, as observed in the cities of Beijing and Seoul, the longtime transmitted flux could be reduced up to 5%. Tropical climates, such as La Parguera or American Samoa, where Precipitable Water in the atmosphere is high ($> 3\text{cm}$), increase the longtime transmitted flux ($\approx 1\%$). Such specific sites are now well-identified and require further study. As opposed to longtime transmitted flux, longtime solar absorptance at the local sites fluctuates less for the most part, showing variations below 1.2%. The variation between the solar transmittance or absorptance values, using the ASTM G173 solar spectrum and the local sites, is different for each sample. Low-e glass samples with a high transmittance variation in the near infrared region are predominantly impacted by these parameters.

In conclusion, the ASTM solar spectrum sometimes overestimates solar transmitted flux. This solar spectrum, modelled with an Air-Mass of 1.5 and clear-sky conditions in the USA, is efficient for most conditions, except for sites near the equator or those which combine high Air-Mass and high atmospheric turbidity. For these locations, we recommend using local atmospheric data whenever possible and available, especially when accurate models and simulations are necessary. Finally, specific low-e and solar control coatings can be designed and manufactured for these specific sites using local atmospheric solar spectra instead of the standard ASTM.

ACKNOWLEDGEMENTS

The research leading to this article has received funding from French national funding from Agence Nationale de la Recherche on the program Investissements d'Avenir (n°ANR-11-EQPX-0014). We would like to thank Sarah Herbelot and Julie Guinebaud for their help with the translation of this article into English.

REFERENCES

- [1] B.P. Jelle, A. Hynd, A. Gustavsen, D. Arasteh, H. Goudey, R. Hart, Fenestration of today and tomorrow: A state-of-the-art review and future research opportunities, *Sol. Energy Mater. Sol. Cells.* 96 (2012) 1–28. <https://doi.org/10.1016/j.solmat.2011.08.010>.
- [2] J. Karlsson, *Windows: optical performance and energy efficiency.*, 2001. <http://uu.diva-portal.org/smash/record.jsf?pid=diva2:161001>.
- [3] G. Feng, B. Dou, X. Xu, D. Chi, Y. Sun, P. Hou, Research on Energy Efficiency Design Key Parameters of Envelope for Nearly Zero Energy Buildings in Cold Area, *Procedia Eng.* 205 (2017) 686–693. <https://doi.org/10.1016/j.proeng.2017.09.885>.
- [4] Tips on Saving Money and Energy in Your Home Contents, (2017). <https://www.energy.gov/energysaver/downloads/energy-saver-guide>.
- [5] S. Amirkhani, A. Bahadori-Jahromi, A. Mylona, P. Godfrey, D. Cook, Impact of Low-E window films on energy consumption and CO₂ emissions of an existing UK hotel building, *Sustain.* 11 (2019). <https://doi.org/10.3390/su11164265>.
- [6] L. Pérez-Lombard, J. Ortiz, C. Pout, A review on buildings energy consumption information, *Energy Build.* 40 (2008) 394–398. <https://doi.org/10.1016/j.enbuild.2007.03.007>.
- [7] A. Gustavsen, B.P. Jelle, D. Arasteh, C. Kohler, *State-of-the-art Highly Insulating Window Frames - Research and Market Review*, 2007.
- [8] ISO 9050 : Glass in building - Determination of lighth transmittance, solar direct transmittance, total solar energy transmittance, ultraviolet transmittance and related glazing factors, (2003).
- [9] H.W. Luo, C.J. Chou, H.S. Chen, M.R. Luo, Museum lighting with LEDs: Evaluation of lighting damage to contemporary photographic materials, *Light. Res. Technol.* 51 (2019) 417–431. <https://doi.org/10.1177/1477153518764538>.
- [10] B.P. Jelle, A. Gustavsen, T.N. Nilsen, T. Jacobsen, Solar material protection factor (SMPF) and solar skin protection factor (SSPF) for window panes and other glass structures in buildings, *Sol. Energy Mater. Sol. Cells.* 91 (2007) 342–354. <https://doi.org/10.1016/j.solmat.2006.10.017>.
- [11] R. Alghamedi, M. Vasiliev, M. Nur-E-Alam, K. Alameh, Spectrally-selective all-inorganic scattering luminophores for solar energy-harvesting clear glass windows, *Sci. Rep.* 4 (2014) 1–9. <https://doi.org/10.1038/srep06632>.
- [12] J. Mohelnikova, Window Glass Coating, *Green Energy Technol.* 33 (2011). <https://doi.org/10.1007/978-0-85729-638-2>.
- [13] H. Altan, J. Mohelnikova, Solar control glass, *Solid State Phenom.* 165 (2010) 1–6. <https://doi.org/10.4028/www.scientific.net/SSP.165.1>.
- [14] S.D. Rezaei, S. Shannigrahi, S. Ramakrishna, A review of conventional, advanced, and smart glazing technologies and materials for improving indoor environment, *Sol. Energy Mater. Sol. Cells.* 159 (2017) 26–51. <https://doi.org/10.1016/j.solmat.2016.08.026>.
- [15] L. Long, H. Ye, How to be smart and energy efficient: A general discussion on thermochromic windows, *Sci. Rep.* 4 (2014) 1–10. <https://doi.org/10.1038/srep06427>.
- [16] M. Arbab, J.J. Finley, Glass in Architecture, *Int. J. Appl. Glas. Sci.* 1 (2010) 118–129. <https://doi.org/10.1111/j.2041-1294.2010.00004.x>.
- [17] *Window Technologies : Glass ,Low-E Coatings, Commercial Windows*, (2015).
- [18] C.A. Gueymard, D. Myers, K. Emery, Proposed reference irradiance spectra for solar

- energy systems testing, *Sol. Energy*. 73 (2002) 443–467. [https://doi.org/10.1016/S0038-092X\(03\)00005-7](https://doi.org/10.1016/S0038-092X(03)00005-7).
- [19] C.A. Gueymard, The SMARTS spectral irradiance model after 25 years: New developments and validation of reference spectra, *Sol. Energy*. 187 (2019) 233–253. <https://doi.org/10.1016/j.solener.2019.05.048>.
- [20] A. Standard, Standard Test Method for Solar Absorptance, Reflectance, and Transmittance of Materials Using Integrating Spheres (E903-12).
- [21] A. Standard, Standard Test Method for Determining Solar or Photopic Reflectance, Transmittance, and Absorptance of Materials Using a Large Diameter Integrating Sphere (E1175), n.d.
- [22] A. Fernández-García, F. Sutter, M. Montecchi, F. Sallaberry, A. Heimsath, C. Heras, E. Le Baron, A. Soum-Glaude, Parameters and method to evaluate the reflectance properties of reflector materials for concentrating solar power technology, *SolarPACES Official Reflectance Guideline Version 3.0*, (2018).
- [23] ISO/CIE 10527:1991(E), CIE standard illuminants for colorimetry, (1991).
- [24] K. Emery, D. Myers, S. Kurtz, What is the appropriate reference spectrum for characterizing concentrator cells?, *Conf. Rec. IEEE Photovolt. Spec. Conf.* (2002) 840–843. <https://doi.org/10.1109/pvsc.2002.1190710>.
- [25] D.R. Myers, K. Emery, C. Gueymard, Proposed reference spectral irradiance standards to improve concentrating photovoltaic system design and performance evaluation, *Conf. Rec. IEEE Photovolt. Spec. Conf.* (2002) 923–926. <https://doi.org/10.1109/pvsc.2002.1190731>.
- [26] C.C. Gonzalez, R.G. Ross, Performance Measurement Reference Conditions for Terrestrial Photovoltaics., *Proc. Annu. Meet. - Am. Sect. Int. Sol. Energy Soc.* 3 . (1980) 1401–1405.
- [27] W. Jessen, S. Wilbert, C.A. Gueymard, J. Polo, Z. Bian, A. Driesse, A. Habte, A. Marzo, P.R. Armstrong, F. Vignola, L. Ramírez, Proposal and evaluation of subordinate standard solar irradiance spectra for applications in solar energy systems, *Sol. Energy*. 168 (2018) 30–43. <https://doi.org/10.1016/j.solener.2018.03.043>.
- [28] A. Vossier, A. Riverola, D. Chemisana, A. Dollet, C. A.Gueymard, Is conversion efficiency still relevant to quality advanced multi-junction solar cells?, *Prog. Photovolt Res. Appl.* (2016) 659–676. <https://doi.org/10.1002/pip>.
- [29] A. Guechi, M. Chegaar, A. Merabet, The effect of water vapor on the performance of solar cells, *Phys. Procedia*. 21 (2011) 108–114. <https://doi.org/10.1016/j.phpro.2011.10.016>.
- [30] B.N. Holben, T.F. Eck, I. Slutsker, D. Tanré, J.P. Buis, A. Setzer, E. Vermote, J.A. Reagan, Y.J. Kaufman, T. Nakajima, F. Lavenu, I. Jankowiak, A. Smirnov, AERONET - A federated instrument network and data archive for aerosol characterization, *Remote Sens. Environ.* 66 (1998) 1–16. [https://doi.org/10.1016/S0034-4257\(98\)00031-5](https://doi.org/10.1016/S0034-4257(98)00031-5).
- [31] D.M. Giles, B.N. Holben, Aeronet, (2021). <https://aeronet.gsfc.nasa.gov/>.
- [32] D.R. Myers, K. Emery, C. Gueymard, Revising and Validating Spectral Irradiance Reference Standards for Photovoltaic Performance Evaluation, *J. Sol. Energy Eng.* 126 (2004) 567. <https://doi.org/10.1115/1.1638784>.
- [33] C.A. Gueymard, SMARTS-2.9.5. For Windows USER ' S MANUAL, Read. (2005).
- [34] C.A. Gueymard, Simple Model of the Atmospheric Radiative Transfer of Sunshine: Algorithms and performance assessment, Florida Sol. Energy Cent. (1995).

- [35] Nasa Earth Observatory, (2017). <http://earthobservatory.nasa.gov/>.
- [36] C.A. Gueymard, Parameterized transmittance model for direct beam and circumsolar spectral irradiance, *Sol. Energy*. 71 (2001) 325–346. [https://doi.org/10.1016/S0038-092X\(01\)00054-8](https://doi.org/10.1016/S0038-092X(01)00054-8).
- [37] D. Chemisana, A. Vossier, L. Pujol, A. Perona, A. Dollet, Characterization of Fresnel lens optical performances using an opal diffuser, *Energy Convers. Manag.* 52 (2011) 658–663. <https://doi.org/10.1016/j.enconman.2010.07.044>.
- [38] C.A. Gueymard, J.A. Ruiz-arias, Validation of direct normal irradiance predictions under arid conditions : A review of radiative models and their turbidity-dependent performance, *Renew. Sustain. Energy Rev.* 45 (2015) 379–396. <https://doi.org/10.1016/j.rser.2015.01.065>.
- [39] H.D. Kumar, D.-P. Häder, H.D. Kumar, D.-P. Häder, Solar Ultraviolet Radiation, *Glob. Aquat. Atmos. Environ.* (1999) 341–376. https://doi.org/10.1007/978-3-642-60070-8_5.
- [40] D.R. Myers, K. Emery, C. Gueymard, Revising and Validating Spectral Irradiance Reference Standards for Photovoltaic Performance Evaluation, *J. Sol. Energy Eng.* 126 (2004) 567. <https://doi.org/10.1115/1.1638784>.
- [41] Scilab, Scilab v5.5.0, (n.d.). <http://www.scilab.org/fr/>.
- [42] A. Grosjean, A. Soum-Glaude, P. Neveu, L. Thomas, Comprehensive simulation and optimization of porous SiO₂ antireflective coating to improve glass solar transmittance for solar energy applications, *Sol. Energy Mater. Sol. Cells*. 182 (2018) 166–177. <https://doi.org/10.1016/J.SOLMAT.2018.03.040>.
- [43] D. Chemisana, Building integrated concentrating photovoltaics: A review, *Renew. Sustain. Energy Rev.* 15 (2011) 603–611. <https://doi.org/10.1016/j.rser.2010.07.017>.
- [44] M. Ferrara, A. Castaldo, S. Esposito, A. D’Angelo, A. Guglielmo, A. Antonaia, AlN–Ag based low-emission sputtered coatings for high visible transmittance window, *Surf. Coatings Technol.* 295 (2016) 2–7. <https://doi.org/10.1016/j.surfcoat.2015.12.015>.
- [45] G. Ding, C. Clavero, Silver-Based Low-Emissivity Coating Technology for Energy-Saving Window Applications, *Intech*. 32 (2013) 137–144.
- [46] M. Oh, S. Tae, S. Hwang, Analysis of heating and cooling loads of electrochromic glazing in high-rise residential buildings in South Korea, *Sustain.* 10 (2018). <https://doi.org/10.3390/su10041121>.
- [47] B.P. Jelle, Solar radiation glazing factors for window panes, glass structures and electrochromic windows in buildings - Measurement and calculation, *Sol. Energy Mater. Sol. Cells*. 116 (2013) 291–323. <https://doi.org/10.1016/j.solmat.2013.04.032>.
- [48] J. Mohelnikova, Nanocoatings for architectural glass, Woodhead Publishing Limited, 2011. <https://doi.org/10.1533/9780857094902.2.182>.
- [49] J. Jaus, C.A. Gueymard, Generalized spectral performance evaluation of multijunction solar cells using a multicore, parallelized version of SMARTS, *AIP Conf. Proc.* 1477 (2012) 122–126. <https://doi.org/10.1063/1.4753849>.
- [50] J.A. Ruiz-Arias, C.A. Gueymard, T. Cebecauer, Direct normal irradiance modeling: Evaluating the impact on accuracy of worldwide gridded aerosol databases, *AIP Conf. Proc.* 2126 (2019). <https://doi.org/10.1063/1.5117710>.
- [51] Solar Gis, (n.d.). <https://solargis.info/> (accessed April 7, 2017).
- [52] Solargis-World-DNI-solar-resource-map-en, (n.d.).
- [53] N.L.A. Chan, H.E. Brindley, N.J. Ekins-Daukes, Impact of individual atmospheric parameters on CPV system power, energy yield and cost of energy, *Prog. Photovoltaics*

Researcj Appl. 5 (n.d.). <https://doi.org/doi: 10.1002/pip.2376>.